DALTON
FULL PAPER

Ruthenium-(II) and -(III) complexes of a ditertiary stibine ligand. The effect of co-ordination on stibine ligand geometry †

Nicholas J. Holmes, William Levason * and Michael Webster

Department of Chemistry, University of Southampton, Southampton, UK SO17 1BJ

Received 7th July 1998, Accepted 20th August 1998

The complexes *trans*-$[RuX_2\{Ph_2Sb(CH_2)_3SbPh_2\}_2]$ (X = Cl, Br or I) have been prepared from $[Ru(dmf)_6][CF_3SO_3]_3$, LiX and the distibine (dmf = dimethylformamide), and characterised by chemical analysis and UV/VIS spectroscopy. They are oxidised by HNO_3 in HBF_4 solution to *trans*-$[RuX_2\{Ph_2Sb(CH_2)_3SbPh_2\}_2]BF_4$. The latter have been characterised by similar techniques, and the Ru^{II}–Ru^{III} redox potentials established electrochemically. The crystal structures of $Ph_2Sb(CH_2)_3SbPh_2$ and *trans*-$[RuBr_2\{Ph_2Sb(CH_2)_3SbPh_2\}_2]\cdot 2CH_2Cl_2$ [Ru–Sb 2.5758(5), 2.6043(8); Ru–Br 2.5770(7) Å] have been determined. Using data from the Cambridge Crystallographic Database on transition metal $SbPh_3$ complexes, the present complexes, and those of $Ph_2SbCH_2SbPh_2$, the effect of co-ordination on the C–Sb–C angles and the Sb–C distances has been examined. A correlation of increased C–Sb–C angles with decreased Sb–C distances is observed on co-ordination.

The majority of knowledge of stibine co-ordination chemistry is based upon $SbPh_3$ and often on isolated complexes included in larger studies of phosphorus and arsenic analogues.[1] A reasonable conclusion drawn from much of this work was that stibines were poorer donors than phosphines, but otherwise formed very similar complexes. Recently, detailed studies have demonstrated that this assumption is invalid, and whilst PR_3 and AsR_3 ligands behave analogously in many systems, significantly different behaviour is exhibited by antimony ligands. Examples are the tendency of stibines to promote higher co-ordination numbers, *e.g.* $[RuCl_2(SbPh_3)_4]$ *versus* $[RuCl_2(PPh_3)_3]$,[2] $[Rh(CO)Cl(SbPh_3)_3]$ *versus* $[Rh(CO)Cl(PPh_3)_2]$,[3] and exclusively five-co-ordination in $[Ni(SbMe_3)_3X_2]$ contrasting with the common four-co-ordination in phosphine complexes;[4] reduced tendency to dissociation in solution in complexes such as $[Cu(SbPh_3)_4]^+$ contrasted with the extensive dissociation in $[Cu(PPh_3)_4]^+$,[5] and the preference for bridging bidentate or η^1 co-ordination by distibinomethanes $R_2SbCH_2SbR_2$, whereas chelation is easily achieved by diphosphinomethanes.[6] Most unusually during our studies of the distibinomethane complexes with metal carbonyls[6,7] we observed that on co-ordination the C–Sb–C bond angles *increase*, whereas C–P–C or C–As–C angles in P or As analogues do not vary significantly between the 'free' and co-ordinated ligands. In the present work we have found a similar effect in complexes of $Ph_2Sb(CH_2)_3SbPh_2$ bonded to platinum metal halides. A survey of reported structures of $SbPh_3$ complexes has also been carried out and the changes in C–Sb–C angles and Sb–C bond lengths examined.

Results and discussion

Ruthenium(II) complexes of 1,3-bis(diphenylstibino)propane, $Ph_2Sb(CH_2)_3SbPh_2$ (dpsp), are easily prepared by reaction of $[Ru(dmf)_6][CF_3SO_3]_3$[8] with dpsp in ethanol in the presence of the appropriate lithium halide. The products $[RuX_2(dpsp)_2]$ (X = Cl, Br or I) are pink or brownish pink solids which are very poorly soluble in common organic solvents including chlorocarbons, acetone and alcohols. Poor solubility is observed in several other series of *trans*-$[RuX_2(L–L)_2]$, *e.g.* L–L = *o*-$C_6H_4(PPh_2)_2$.[9] The identification of $[RuX_2(dpsp)_2]$ as *trans* isomers follows from the diffuse reflectance UV/VIS spectra (Table 1) which show two weak d–d bands, and was confirmed by the crystal structure of the bromide complex described below. Although a full ligand field analysis of the spectra of low-spin d^6 complexes is not possible when only the two lowest energy bands are observed, comparison of the transition energies with those in *trans*-$[RuX_2(L–L)_2]$ (L–L = $Ph_2PCH_2CH_2PPh_2$ or $Ph_2AsCH_2CH_2AsPh_2$; X = Cl, Br or I) (Table 1)[9,10] shows that as expected the distibine exerts a weaker ligand field.

Oxidation of the *trans*-$[RuX_2(dpsp)_2]$ to the more deeply coloured *trans*-$[RuX_2(dpsp)_2]BF_4$ was achieved by stirring a suspension in 40% HBF_4 with concentrated HNO_3. In contrast to the ruthenium(II) complexes, the Ru^{II} cations are easily soluble in organic solvents, although the solutions decompose slowly on standing. The UV/VIS spectra (Table 1) are typical of *trans*-$[RuX_2(L–L)_2]^+$ complexes,[9,11] the major features being assignable to L(or X)→Ru charge transfer transitions, which are expected to extend into the near IR region in ruthenium(III)–stibine complexes.[2] Cyclic voltammetric data reveal reversible 1e reductions in CH_2Cl_2 solution, the Ru^{II}–Ru^{III} potentials (Table 1) being somewhat more positive than those observed for aryl substituted diphosphine or diarsine ruthenium complexes.[9] The potentials are less positive than observed in *trans*-$[RuX_2(SbPh_3)_4]^{0/+}$,[2] but identical to those seen in *trans*-$[RuX_2(SbMe_2Ph)_4]^{0/+}$.[12] The dependence of the redox potential on both the donor atom and the R groups on the Group 15 ligands is typical of a wide range of ruthenium and osmium complexes.

Crystal structures of $Ph_2Sb(CH_2)_3SbPh_2$ and $[RuBr_2\{Ph_2Sb(CH_2)_3SbPh_2\}_2]\cdot 2CH_2Cl_2$

The structure of $Ph_2Sb(CH_2)_3SbPh_2$ is shown in Fig. 1 with selected bond lengths and angles in Table 2. The structure confirms the chemical proposal and shows unexceptional bond lengths. The features of interest are the *trans* conformation of the C_3 backbone shown in the torsion angles and the C–Sb–C angles which will be referred to again when discussing the complex.

The ruthenium complex is a centrosymmetric *trans* isomer (see Fig. 2 and Table 2). The Ru–Br bond length 2.5770(7) Å

† *Supplementary data available*: Cambridge Structural Database 'refcodes' of the compounds used as well as the bond lengths and angles of all the fragments. For direct electronic access see http://www.rsc.org/suppdata/dt/1998/3457/, otherwise available from BLDSC (No. SUP 57433, 5 pp.) or the RSC Library. See Instructions for Authors, 1998, Issue 1 (http://www.rsc.org/dalton).

Table 1 Selected spectroscopic data

Complex	Colour	$\tilde{\nu}_{max}/10^3$ cm^{-1} (ε_{mol}/dm^3 mol^{-1} cm^{-1})[a]	E°[b]/V	m/z[c]
$[RuCl_2(dpsp)_2]$	Light pink	33.0, 27.9 (sh), 19.2[d]		
$[RuBr_2(dpsp)_2]$	Light purple	35.7, 31.8, 25.5 (sh), 18.9[d]		
$[RuI_2(dpsp)_2]$	Light brown	32.6, 28.0, 22.8 (sh), 18.5[d]		
$[RuCl_2(dpsp)_2]BF_4$	Dark orange	33.8 (48500), 29.7 (22040), 21.0 (sh) (1160), 11.1 (756)	+0.63	1360 (1356)
$[RuBr_2(dpsp)_2]BF_4$	Red-purple	30.5 (sh) (26550), 28.2 (31950), 22.0 (1610), 20.4 (sh) (1500), 10.4 (1660)	+0.66	1450 (1444)
$[RuI_2(dpsp)_2]BF_4$	Green-brown	32.6 (17060), 29.4 (11200), 26.2 (sh) ((6200), 18.4 (sh) (740), 10.7 (290), 8.7 (985)	+0.68	1544 (1540)
$[RuCl_2(Ph_2PCH_2CH_2PPh_2)_2]$[e]		26.2 (160), 22.3 (80)		
$[RuBr_2(Ph_2PCH_2CH_2PPh_2)_2]$[e]		26.6 (290), 21.6 (150)		
$[RuI_2(Ph_2PCH_2CH_2PPh_2)_2]$[e]		27.1 (930), 22.1 (470)		
$[RuCl_2(Ph_2AsCH_2CH_2AsPh)_2]$[e]		26.0 (220), 21.6 (130)		
$[RuI_2(Ph_2AsCH_2CH_2AsPh_2)_2]$[e]		25.0 (sh), 19.2 (475)		

[a] In CH_2Cl_2 solution unless indicated otherwise. [b] Redox potential in CH_2Cl_2 containing $[^nBu_4N]BF_4$, relative to Fc–Fc$^+$ +0.56 V. [c] Electrospray mass spectrum, calculated peak for $[RuX_2(dpsp)_2]^+$ in parentheses based upon ^{35}Cl, ^{79}Br, ^{102}Ru and ^{121}Sb isotopes. [d] Diffuse reflectance. [e] Data from refs. 8 and 9.

Table 2 Selected bond lengths (Å) and angles (°) for $Ph_2Sb(CH_2)_3SbPh_2$ and $[RuBr_2\{Ph_2Sb(CH_2)_3SbPh_2\}_2]\cdot 2CH_2Cl_2$

(a) $Ph_2Sb(CH_2)_3SbPh_2$			
Sb(1)–C(1)	2.156(5)	Sb(2)–C(15)	2.155(6)
Sb(1)–C(7)	2.154(6)	Sb(2)–C(16)	2.160(6)
Sb(1)–C(13)	2.158(6)	Sb(2)–C(22)	2.141(7)
C(13)–C(14)	1.524(8)	C(14)–C(15)	1.531(8)
C–C (phenyl)	1.36(1)–1.413(8)	C–H	0.84–1.20
C(1)–Sb(1)–C(7)	96.4(2)	C(15)–Sb(2)–C(16)	96.0(2)
C(1)–Sb(1)–C(13)	95.9(2)	C(15)–Sb(2)–C(22)	94.3(2)
C(7)–Sb(1)–C(13)	93.1(2)	C(16)–Sb(2)–C(22)	97.0(2)
Sb(1)–C(13)–C(14)	113.4(4)	C(13)–C(14)–C(15)	110.9(5)
Sb(2)–C(15)–C(14)	111.7(4)		
C(1)–Sb(1)–C(13)–C(14)	177.9(5)	C(7)–Sb(1)–C(13)–C(14)	81.1(5)
Sb(1)–C(13)–C(14)–C(15)	−175.8(4)	C(13)–C(14)–C(15)–Sb(2)	−176.4(4)
C(14)–C(15)–Sb(2)–C(16)	173.6(5)	C(14)–C(15)–Sb(2)–C(22)	76.1(5)
(b) $[RuBr_2\{Ph_2Sb(CH_2)_3SbPh_2\}_2]\cdot 2CH_2Cl_2$			
Ru–Sb(1)	2.5758(5)	Ru–Br	2.5770(7)
Ru–Sb(2)	2.6043(8)	Sb(1)···Sb(2)	3.607
Sb(1)–C(1)	2.149(7)	Sb(2)–C(15)	2.146(7)
Sb(1)–C(7)	2.127(7)	Sb(2)–C(16)	2.148(7)
Sb(1)–C(13)	2.164(7)	Sb(2)–C(22)	2.146(7)
C(13)–C(14)	1.52(1)	C(14)–C(15)	1.52(1)
C–C (phenyl)	1.36(1)–1.42(1)	C–H	0.92–1.19
Br–Ru–Sb(1)	86.20(2)	Sb(1)–Ru–Sb(2)	88.25(2)
Br–Ru–Sb(2)	80.74(2)		
Ru–Sb(1)–C	117.2(2)–119.1(2)	Ru–Sb(2)–C	115.3(2)–124.1(2)
C(1)–Sb(1)–C(7)	102.3(3)	C(15)–Sb(2)–C(16)	97.2(3)
C(1)–Sb(1)–C(13)	96.5(3)	C(15)–Sb(2)–C(22)	96.6(3)
C(7)–Sb(1)–C(13)	99.4(3)	C(16)–Sb(2)–C(22)	100.2(3)
Sb(1)–C(13)–C(14)	118.7(5)	C(13)–C(14)–C(15)	115.4(6)
Sb(2)–C(15)–C(14)	114.9(5)		
C(1)–Sb(1)–C(13)–C(14)	170.1(5)	C(7)–Sb(1)–C(13)–C(14)	−86.2(6)
Sb(1)–C(13)–C(14)–C(15)	−67.5(7)	C(13)–C(14)–C(15)–Sb(2)	76.6(7)
C(14)–C(15)–Sb(2)–C(16)	172.5(5)	C(14)–C(15)–Sb(2)–C(22)	71.3(6)

may be compared with those in *trans*-$[RuBr_2(SbMe_2Ph)_4]$[12] [2.572(1), 2.567(1) Å], but is significantly longer than that in the ruthenium(III) complex *trans*-$[RuBr_2\{o\text{-}C_6F_4(AsMe_2)_2\}_2]BF_4$ [2.455(1) Å].[9] Similarly the Ru–Sb distances of 2.5758(5), 2.6043(8) Å compare with those in *trans*-$[RuBr_2(SbMe_2Ph)_4]$[12] [2.573(1)–2.596(1) Å], *trans*-$[RuCl_2(SbPh_3)_4]$[2] [2.625(1)–2.632(1) Å], and with the Rh–Sb distances [2.594(2), 2.611(2) Å] in *trans*-$[RhCl_2(dpsp)_2]ClO_4$.[13] The C–Sb–C angles in the free dpsp range (Table 2) from 93.1(2) to 97.0(2)° [average 95.4(1.5)°‡] which on comparison with those in *trans*-$[RuBr_2(dpsp)_2]$ [96.5(3)–102.3(3), average 98.7(2.3)°] and in *trans*-$[RhCl_2(dpsp)_2]ClO_4$ [98(1)–106(1), average = 100(3)°] show that a significant increase in the C–Sb–C angles occur in complexes of dpsp, as is the case for the distibinomethane complexes.[6,7] The angle changes in the antimony environment might also be associated with changes in the bond lengths, and the structural parameters (Table 2) were examined to see if d(Sb–C) changed upon co-ordination. In free dpsp the average Sb–C bond length is 2.154(6) Å whereas in *trans*-$[RuBr_2(dpsp)_2]$ the average Sb–C distance is 2.147(11) Å and in *trans*-$[RhCl_2(dpsp)_2]ClO_4$, 2.135(28) Å.[13] Thus in this limited series of complexes the data hint that on co-ordination to a metal the Sb–C bonds shorten marginally. Re-examination of the distibinomethane data[6,7]

‡ In this and subsequent average values, an unweighted mean was used and the figures in parentheses represent the sample standard deviation.

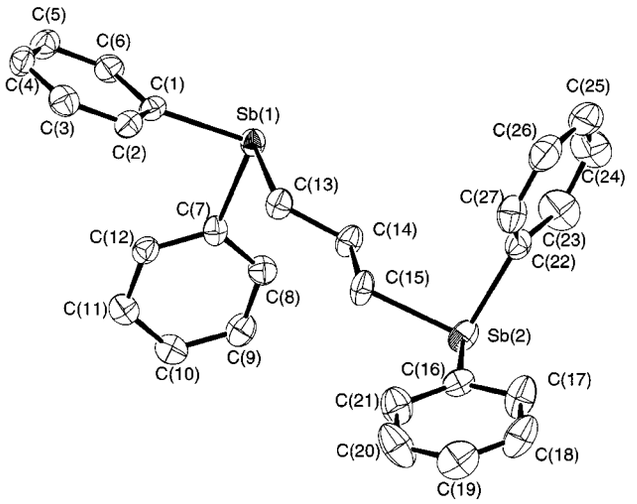

Fig. 1 The ligand $Ph_2Sb(CH_2)_3SbPh_2$ showing the atom numbering scheme. Thermal ellipsoids are drawn at the 50% probability level and H atoms omitted for clarity.

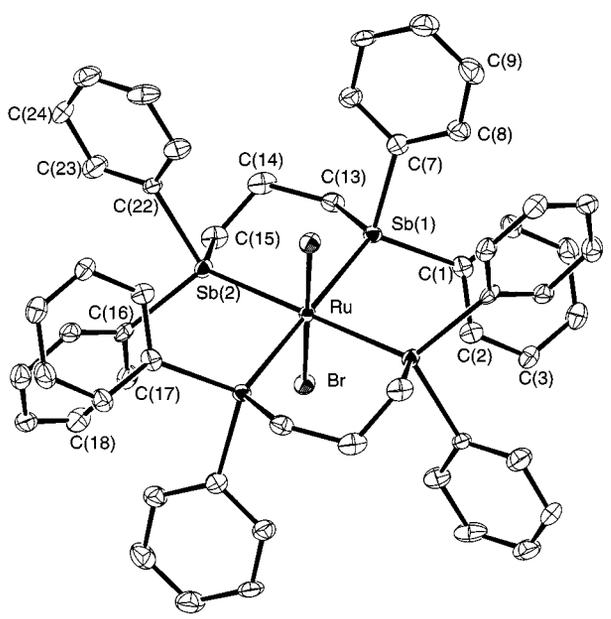

Fig. 2 The structure of $[RuBr_2\{Ph_2Sb(CH_2)_3SbPh_2\}_2]$ showing the atom numbering scheme. Details as in Fig. 1.

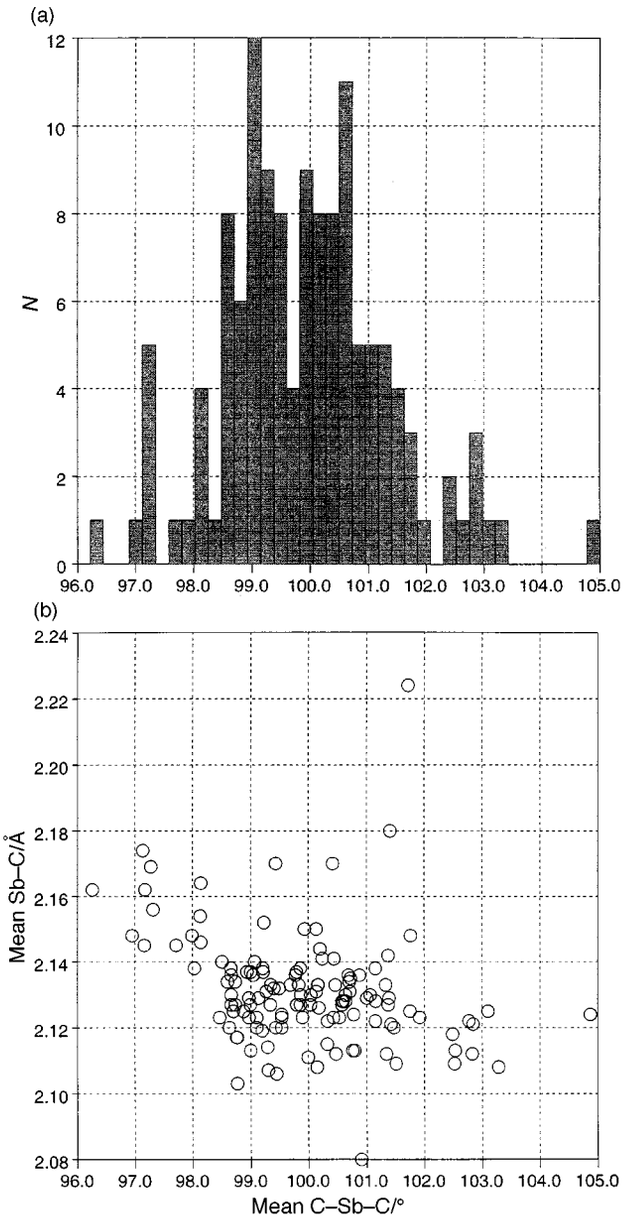

Fig. 3 (a) Histogram showing the average C–Sb–C angle (°) for Ph_3Sb-E residues where E = transition element. (b) Scattergram plot of the average C–Sb–C angle (°) against the average Sb–C bond length (Å) for Ph_3Sb–E residues where E = transition element.

also suggests a similar effect, although in both cases the changes are much less obvious than the angle variations.

To place these observations on a firmer foundation a much larger number of examples are required. Moreover X-ray structural data on the 'free' ligand is needed in each case, which eliminates consideration of, for example, recently reported complexes with $SbMe_2Ph$[12] or $SbPr^i_3$[14] where the ligands are air-sensitive oils for which bond length/angle data are not available. Thus we concentrated upon complexes of $SbPh_3$ using the Cambridge Structural Database (CSD)[15,16] and also included several recent structures (see SUP 57433) not yet available from the database.

Geometric effects of co-ordination in $SbPh_3$ complexes

A number of authors have exploited the large amount of data in the CSD to seek generalisations and patterns in structures.[17,18] In the present case for each structural fragment Ph_3Sb–E where E is a transition element, the three C–Sb–C angles and a mean C–Sb–C angle were obtained for compounds in the database.[19] This yielded 86 'hits' which together with some 16 other compounds (44 fragments) which had not yet entered the compilation gave 130 fragments available for the analysis. The acceptance criteria were that $R < 10\%$ and that co-ordinates were available. A histogram of the mean angle for 129 entries (excluding CAJZUI which is clearly in error) [Fig. 3(a)] shows the distribution with a mean of 99.9° and sample e.s.d. of 1.4°. There are three structures[20–22] of 'free' Ph_3Sb giving rise to five fragments of uncomplexed ligand for which the mean angle is 96.27(0.21)°. By inspection of Fig. 3(a) there is an increase in the C–Sb–C angle on co-ordination and in an effort to quantify this the Student's *t*-test was carried out for the case of unequal sample variances[23] giving $t = 22.7$ (29 degrees of freedom) from which we conclude, in statistical terms, that the difference in the sample means is highly significant at $\alpha < 0.001$.

Along with the angle data, the Sb–C bond lengths, a mean Sb–C bond length, and the Sb–E distance were tabulated for each fragment. A scattergram plot of mean C–Sb–C against d(Sb–E) showed no recognisable pattern whereas the scattergram of mean C–Sb–C against mean Sb–C distance for our 129 sample points showed that larger angles are associated with shorter Sb–C distances [Fig. 3(b)]. The variation in mean bond

Table 3 Crystallographic details *

	$Ph_2Sb(CH_2)_3SbPh_2$	$[RuBr_2\{Ph_2Sb(CH_2)_3SbPh_2\}_2]\cdot 2CH_2Cl_2$
Formula	$C_{27}H_{26}Sb_2$	$C_{56}H_{56}Br_2Cl_4RuSb_4$
M_r	594.00	1618.75
Space group	$C2/c$ (no. 15)	$P2_1/n$ (no. 14)
a/Å	18.982(3)	11.561(3)
b/Å	8.243(5)	15.950(4)
c/Å	30.163(3)	15.245(3)
β/°	90.75(1)	92.90(2)
U/Å^3	4719(2)	2807.3(9)
2θ Range for cell/°	21.0–28.0 (24 refs.)	48.5–49.9 (25 refs.)
D_c/g cm^{-3}	1.672	1.915
Z	8	2
$F(000)$	2320	1556
Crystal size/mm	0.52 × 0.35 × 0.10	0.38 × 0.35 × 0.30
Total observations	4627	5414
No. unique (R_{int})	4479 (0.024)	5146 (0.028)
hkl Range	0–22, 0–9, −35 to 35	0–13, 0–18, −18 to 18
Maximum, minimum transmission	1.000, 0.552	1.000, 0.847
No. data in refinement	3090 [$I > 2.5\sigma(I)$]	4272 [$I > 2\sigma(I)$]
No. parameters	262	304
μ/cm^{-1}	23.14	38.14
S	1.51	3.26
Maximum shift/e.s.d.	0.01	0.02
Residual electron density/e Å^{-3}	−0.52 to +1.81	−1.77 to +1.06
R [$I > n\sigma(I)$]	0.032 (n = 2.5)	0.037 (n = 2.0)
R' [$I > n\sigma(I)$]	0.034 (n = 2.5)	0.043 (n = 2.0)

* In common: monoclinic; T = 150 K; scan mode ω–2θ; absorption correction ψ scan (3 reflections); $w^{-1} = \sigma^2(F_o)$; maximum $2\theta = 50°$; $R = \Sigma\,||F_o| - |F_c||/\Sigma|F_o|$; $R' = [\Sigma w(F_o - F_c)^2/\Sigma w F_o^2]^{\frac{1}{2}}$.

length is not large (0.14 Å) and excluding two outliers (both BITXIL) even smaller (0.08 Å); often there are quite large errors associated with individual Sb–C distances in the reported structures. The 'free' ligand [mean C–Sb–C 96.27(21)°, mean Sb–C 2.150(7) Å] can be seen to follow the same trend. For the bond length/bond angle data in Fig. 3(b), the product moment correlation coefficient (−0.30) and the Spearman rank correlation coefficient (−0.32) for our 129 sample points are similar in value. The significance of the latter has been tested and on the null hypothesis can be rejected at better than the $\alpha = 0.005$ (for the one-tailed test). The use of non-parametric statistical tests in chemical problems has been briefly discussed.[24] For a similar sized sample of Ph_3As complexes with transition elements, the C–As–C angle also increases on co-ordination [mean C–As–C: 102.3(1.3) (complex); 99.9(4)° ('free' ligand)], but the scattergram analogous to Fig. 3(b) was less convincing. For compounds of As and Sb there were few examples where E was not a transition element. A detailed analysis of a much larger sample (1860) of Ph_3P–E fragments where E includes a wide range of transition and main group elements has been reported by Orpen and co-workers.[24] In this a similar relationship between the mean C–P–C angle and mean P–C bond length was convincingly established and it now appears as though this is a feature of Group 15 Ph_3P and Ph_3Sb and possibly Ph_3As complexes. Orpen and co-workers[24] observed that "In general, structures in which E is a transition-series element show PPh_3 geometries close to that of triphenylphosphine itself". In the case of the stibines, the range of metals (E) is smaller, the majority of the complexes belonging to Groups 8–11 (see SUP 57433), but it is notable that the average C–Sb–C angles are **all** larger than in the 'free' ligand.

There are several possible rationalisations of these effects. On the VSEPR model, co-ordination of the $SbPh_3$ to a metal converts the lone pair into a bond pair, and hence would reduce repulsions at the antimony, which could lead to an increase in C–Sb–C angles. However such effects would be expected to be greater at smaller atoms like phosphorus, and so we tend to discount this explanation. On a hybridisation model, the increasing C–Sb–C angles on co-ordination correspond to increased s character in the Sb–C bond (and correspondingly increased p character in the "lone pair" co-ordinating to the metal centre). On a Walsh diagram approach[24] σ donation of the antimony lone pair on co-ordination should result in a decreased population of the lone-pair orbital, (decreased drive towards pyramidalisation) and hence increased C–Sb–C angles and decreased Sb–C distances, as observed. It is also notable that any π-back bonding into Sb–C σ* orbitals should tend to decrease the C–Sb–C angles and increase Sb–C. On this basis, the results support the view that stibines are poor π acceptors (certainly poorer than phosphines), even in low oxidation state metal complexes.[1] Finally relativistic effects are likely to be significant for the antimony 5s electrons. A more detailed understanding of the angle variation upon co-ordination must await high level molecular orbital calculations which are presently largely lacking in organoantimony chemistry.[25] We also note in passing that in $BiPh_3$ complexes the C–Bi–C angles increase on co-ordination, although here the data are limited to four(!) crystal structures.[26]

Experimental

Physical measurements were made as described elsewhere.[7,12] The ligand was made by the literature method.[27]

Preparations

$[RuX_2\{Ph_2Sb(CH_2)_3SbPh_2\}_2]$, X = Cl, Br or I. The compounds $[Ru(dmf)_6](CF_3SO_3)_3$[8] (0.1 mmol) and $Ph_2Sb(CH_2)_3SbPh_2$ (0.2 mmol) were refluxed in ethanol (20 ml) for 10 min; LiX (0.2 mmol) in warm ethanol (5 ml) was added and the solution refluxed for 10 min. On cooling the solid produced was filtered off, washed with ethanol (2 × 10 ml) and dried *in vacuo*. Yields 70–80% (X = Cl. Found: C, 47.1; H, 3.3. Calc. for $C_{54}H_{52}Cl_2RuSb_4$: C, 47.6; H, 3.8. X = Br. Found: C, 44.3; H, 3.7. Calc. for $C_{54}H_{52}Br_2RuSb_4$: C, 44.7; H, 3.6. X = I. Found: C, 41.6; H, 3.0. Calc. for $C_{54}H_{52}I_2RuSb_4$: C, 42.0; H, 3.4%).

$[RuX_2\{Ph_2Sb(CH_2)_3SbPh_2\}_2][BF_4]$, X = Cl, Br or I. The compound $[RuX_2\{Ph_2Sb(CH_2)_3SbPh_2\}_2]$ was suspended in 40% HBF_4 (20 ml) cooled in an ice-bath. Concentrated HNO_3 (several drops) was added with rapid stirring and after 30 min the solid was filtered off, washed with water (2 × 10 ml) and

dried *in vacuo*. Yields 90–95% (X = Cl. Found: C, 44.4; H, 3.7. Calc. for $C_{54}H_{52}BCl_2F_4RuSb_4$: C, 44.8; H, 3.6. X = Br. Found: C, 42.4; H, 3.6. Calc. for $C_{54}H_{52}BBr_2F_4RuSb_4$: C, 42.2; H, 3.4%. X = I. Found: C, 40.0; H, 2.9. Calc. for $C_{54}H_{52}BF_4I_2RuSb_4$: C, 39.8; H, 3.2%).

Crystallography

Crystals of $Ph_2Sb(CH_2)_3SbPh_2$ were obtained from CH_2Cl_2 by cooling to −20 °C. Pink crystals of *trans*-$[RuBr_2(dpsp)_2]\cdot 2CH_2Cl_2$ grew from a solution of *trans*-$[RuBr_2(dpsp)_2]BF_4$ in CH_2Cl_2 during vapour diffusion of diethyl ether. Since the *trans*-$[RuBr_2(dpsp)_2]$ is insoluble in CH_2Cl_2 the crystals form by slow decomposition of the ruthenium(III) compound. Other crystals in the same batch were confirmed as the ruthenium(II) complex by comparison of their spectra with those of genuine samples. Details of the crystallographic studies are presented in Table 3. Data were collected on a Rigaku AFC7S diffractometer equipped with Mo-Kα radiation ($\lambda = 0.71073$ Å) and a graphite monochromator. Selected crystals were mounted in oil on glass fibres and held at 150 K using an Oxford Cryosystems low temperature device. No decay was observed in the check reflections during the data collection. Structure solution was by means of DIRDIF[28] followed by full-matrix least-squares refinement on *F* using the TEXSAN package.[29] The systematic absences for $Ph_2Sb(CH_2)_3SbPh_2$ gave the space group as *Cc* or *C*2/*c* with the latter favoured by the *N*(*z*) test and confirmed by the structure solution. A solvent molecule became apparent in the structure of the complex and was included in the model. Later electron density maps revealed the position of all of the H atoms (except those of the CH_2Cl_2) and they were included but not refined. Residual peaks in the electron density maps were close to heavy atoms.

CCDC reference number 186/1130.

Acknowledgements

We thank the EPSRC for support (to N. J. H.), for funds to purchase the X-ray diffractometer and for access to the Chemical Database Service at the Daresbury Laboratory.

References

1 N. R. Champness and W. Levason, *Coord. Chem. Rev.*, 1993, **133**, 115.
2 N. R. Champness, W. Levason and M. Webster, *Inorg. Chim. Acta*, 1993, **208**, 189.
3 P. E. Garrou and G. E. Hartwell, *J. Organomet. Chem.*, 1974, **69**, 445.
4 M. F. Ludmann, M. Dartiguenave and Y. Dartiguenave, *Inorg. Chem.*, 1977, **16**, 440.
5 J. R. Black, W. Levason, M. D. Spicer and M. Webster, *J. Chem. Soc.*, *Dalton Trans.*, 1993, 3129.
6 A. M. Hill, W. Levason, M. Webster and I. Albers, *Organometallics*, 1997, **16**, 5641.
7 A. M. Hill, N. J. Holmes, A. R. J. Genge, W. Levason, M. Webster and S. Rutschow, *J. Chem. Soc.*, *Dalton Trans.*, 1998, 825.
8 R. J. Judd, R. Cao, M. Biner, T. Armbruster, H.-B. Bürgi, A. E. Merbach and A. Ludi, *Inorg. Chem.*, 1995, **34**, 5080.
9 N. R. Champness, W. Levason, D. Pletcher and M. Webster, *J. Chem. Soc.*, *Dalton Trans.*, 1992, 3243.
10 N. R. Champness, M.Phil. Thesis, University of Southampton, 1990.
11 N. R. Champness, W. Levason, S. R. Preece, M. Webster and C. S. Frampton, *Inorg. Chim. Acta*, 1996, **244**, 65.
12 N. J. Holmes, W. Levason and M. Webster, *J. Chem. Soc.*, *Dalton Trans.*, 1997, 4223.
13 A. M. Hill, W. Levason and M. Webster, *Inorg. Chim. Acta*, 1998, **271**, 203.
14 H. Werner, C. Grünwald, M. Laubender and O. Gevert, *Chem. Ber.*, 1996, **129**, 1191; C. Grünwald, M. Laubender, J. Wolf and H. Werner, *J. Chem. Soc.*, *Dalton Trans.*, 1998, 833.
15 F. H. Allen and O. Kennard, *Chem. Des. Autom. News*, 1993, **8**, 1 and 31.
16 D. A. Fletcher, R. F. McMeeking and D. Parkin, *J. Chem. Inf. Comput. Sci.*, 1996, **36**, 746.
17 F. H. Allen and O. Kennard, in *Crystallographic Databases*, eds. F. H. Allen, G. Bergerhoff and R. Sievers, International Union of Crystallography, Chester, 1987.
18 A. G. Orpen, *Chem. Soc. Rev.*, 1993, **22**, 191.
19 Cambridge Structural Database, version 5.15, release April 1998 (181,309 entries), accessed through the Chemical Database Service at the Daresbury Laboratory and using the QUEST and VISTA software.
20 E. A. Adams, J. W. Kolis and W. T. Pennington, *Acta Crystallogr.*, *Sect. C*, 1990, **46**, 917.
21 M. Fedurco, M. M. Olmstead and W. R. Fawcett, *Inorg. Chem.*, 1995, **34**, 390.
22 Effendy, W. J. Grigsby, R. D. Hart, C. L. Raston, B. W. Skelton and A. H. White, *Aust. J. Chem.*, 1997, **50**, 675.
23 Microsoft Excel, version 5.0, Microsoft Corporation, USA, 1993–1994.
24 B. J. Dunne, R. B. Morris and A. G. Orpen, *J. Chem. Soc.*, *Dalton Trans.*, 1991, 653.
25 S. Nagase, in *The Chemistry of Organic Arsenic, Antimony and Bismuth Compounds*, ed. S. Patai, Wiley, New York 1994, ch. 1.
26 N. J. Holmes, W. Levason and M. Webster, *J. Organomet. Chem.*, 1997, **545–546**, 111.
27 S. Sato, Y. Matsumura and R. Okawara, *J. Organomet. Chem.*, 1972, **43**, 333.
28 P. T. Beurskens, G. Admiraal, G. Buerskens, W. P. Bosman, S. Garcia-Granda, R. O. Gould, J. M. M. Smits and C. Smykalla, The DIRDIF program system, University of Nijmegen, 1992.
29 TEXSAN, Single crystal structure analysis software, version 1.7-1, Molecular Structure Corporation, The Woodlands, TX, 1995.

Paper 8/05245J